



OPEN

Comparison between blue-on-yellow and white-on-white perimetry in patients with branch retinal vein occlusion

Kunihiro Azuma¹, Tatsuya Inoue^{1,2✉}, Ryosuke Fujino¹, Nozomi Igarashi¹, Shotaro Asano¹, Yoko Nomura¹, Yohei Hashimoto¹, Keiko Azuma¹, Ryo Asaoka^{1,3,4}, Kazuaki Kadonosono² & Ryo Obata¹

This study aimed to compare blue-on-yellow (B/Y) perimetry with white-on-white (W/W) perimetry in eyes with branch retinal vein occlusion (BRVO). The following measurements were performed in 29 eyes of 29 patients with resolved BRVO: W/W and B/Y perimetries using 10-2 test grid, retinal volume (RV) using optical coherence tomography (OCT), and vessel densities (VD) of the superficial capillary layer (VDs) and deep capillary layer (VDd) using OCT angiography (OCTA). First, the difference in the retinal sensitivity (RS) between BRVO-affected and unaffected areas was compared between RS_B/Y and RS_W/W in the parafoveal and extrafoveal areas. Moreover, the structure–function relationship between vessel density and RS was compared between B/Y and W/W perimetries (RS_B/Y and RS_W/W, respectively). The difference in RS between BRVO-affected and unaffected areas was significantly larger with RS_B/Y than with RS_W/W in both the parafoveal and extrafoveal areas. In the parafoveal area, VDs, VDd, and RV were significantly correlated with both RS_W/W and RS_B/Y. In contrast, in the extrafoveal area, only VDd was included in the optimal models. Our findings suggest that RS_B/Y more strongly reflects the anatomical structure and BRVO-affected area.

Branch retinal vein occlusion (BRVO) is one of the common retinal vascular diseases in the clinical setting. Eyes affected with BRVO often develop a retinal capillary nonperfused area (NPA) that may lead to neovascularization and vitreous hemorrhage¹. Fluorescein angiography has been the gold standard to detect NPA; however, more detailed evaluation of the retinal vessels is now possible using the recently developed method of optical coherence tomography angiography (OCTA)². The superficial and deep retinal vasculatures can be observed separately using the *en face* visualization technique³. Recent studies have revealed that the retinal vessels are associated with visual function in eyes with BRVO. In a study by Wakabayashi et al., the microvasculature of the vascular perfusion area in the deep capillary plexus within a 3 × 3-mm macular area was found to be strongly correlated with visual acuity in eyes with resolved BRVO⁴. Another study suggested that there is a significant reduction in retinal sensitivity (RS) in NPA measured using OCTA in eyes with BRVO⁵.

Blue-on-yellow (B/Y) perimetry uses a short-wavelength blue stimulus on a high-luminance yellow background that can be used to evaluate the function of blue cones by isolating them from the other cones. Early detection of glaucomatous visual field (VF) damage is one of the most representative merits of B/Y perimetry compared with the conventional white-on-white (W/W) perimetry^{6–8}. Furthermore, B/Y perimetry has reportedly been advantageous in detecting early abnormalities in many fundus diseases, such as diabetic retinopathy, optic nerve disorders, and central serous chorioretinopathy^{9–13}. However, to the best of our knowledge, there have been few studies on BRVO using B/Y perimetry.

¹Department of Ophthalmology, The University of Tokyo, Tokyo, Japan. ²Department of Ophthalmology and Micro-Technology, Yokohama City University, 4-57 Urafune, Minami-ku, Yokohama 232-0024, Japan. ³Department of Ophthalmology, Seirei Hamamatsu General Hospital, Shizuoka, Hamamatsu, Japan. ⁴Seirei Christopher University, Shizuoka, Hamamatsu, Japan. ✉email: inouet-tky@umin.ac.jp

Variable	Mean \pm SD	Range
Eyes (phakia/pseudophakia)	29 (23/6)	
Age (years)	68.3 \pm 9.53	52–85
Gender (male to female)	11:18	
logMAR VA	0.057 \pm 0.18	–0.079 to 0.82
Mean retinal sensitivity in W/W perimetry (dB)	29.58 \pm 2.1	25.1–32.92
Mean retinal sensitivity in B/Y perimetry (dB)	23.11 \pm 3.77	17.15–29.27
CRT (μ m)	268.17 \pm 33.57	197–364
CCT (μ m)	171.55 \pm 34.70	75–238

Table 1. Baseline characteristics of the patients. *logMAR VA* logarithm of the minimum angle resolution visual acuity, *CRT* central retinal thickness, *CCT* central choroidal thickness.

	RS_W/W (dB)	RS_B/Y (dB)	VDs (%)	VDd (%)	RV (mm ³)
Parafovea	30.15 \pm 3.19 (11.5–34.25)	23.54 \pm 5.25 (2.17–32)	81.41 \pm 6.79 (61.40–95.71)	86.68 \pm 8.25 (60.88–98.92)	0.5 \pm 0.05 (0.31–0.63)
Extrafovea	28.82 \pm 3.48 (14.50–33.10)	22.85 \pm 5.17 (1.33–30.90)	77.47 \pm 6.56 (59.70–92.88)	81.75 \pm 8.78 (50.00–98.14)	1.53 \pm 0.12 (1.23–1.88)
Center	30.37 \pm 2.87 (19.75–33.75)	22.37 \pm 4.99 (3.75–28.50)	67.68 \pm 6.12 (54.49–78.59)	63.86 \pm 7.19 (46.42–74.67)	0.21 \pm 0.03 (0.15–0.29)
Total	29.58 \pm 2.1 (25.09–32.92)	23.11 \pm 3.77 (13.19–29.59)	78.13 \pm 4.04 (69.59–84.25)	81.93 \pm 5.42 (69.46–90.27)	0.93 \pm 0.05 (0.82–1.02)

Table 2. Mean value of each measurement. *RS_W/W* retinal sensitivity in white-on-white perimetry, *RS_B/Y* retinal sensitivity in blue-on-yellow perimetry, *VDs* vessel density in superficial capillary plexus, *VDd* vessel density in deep capillary plexus, *RV* retinal volume.

Therefore, this study aimed to compare B/Y perimetry and W/W perimetry in eyes with BRVO and perform a detailed analysis of the structure–function relationship between vessel density (VD) and RS using both perimetries.

Results

A total of 29 eyes of 29 patients with resolved BRVO were enrolled in this study. Baseline characteristics of the subjects are presented in Table 1. All the patients had hypertension but not hyperlipidemia. There were 17 eyes with major BRVO and 12 with macular BRVO.

The values of the retinal sensitivity measured using W/W and B/Y perimetries (*RS_W/W* and *RS_B/Y*, respectively), VD in the superficial capillary plexus (SCP) and deep capillary plexus (DCP) measured using OCTA (*VDs* and *VDd*, respectively), and retinal volume (*RV*) are presented in Table 2. The correlation between functional measurement and OCT parameters was analyzed using 6-mm Early Treatment of Diabetic Retinopathy Study (ETDRS) grid. Three eyes had central macular nonperfusion, and the other 26 eyes had central macular perfusion. The representative image of an eye with central macular nonperfusion is shown in Supplementary Figure S1.

The results of the univariate analysis between the best-corrected visual acuity (BCVA) and other parameters in the center and parafovea are presented in Supplementary Table S1. No parameters were significantly related to BCVA in the central area. In the parafovea, *VDs* and *RV* were significantly correlated to BCVA (linear model, $P=0.037$ and $P=0.011$, respectively). Based on the second-order bias-corrected Akaike Information Criterion (AICc) model selection for BCVA, only the parafoveal *RV* was selected as the explanatory variable (AICc = –16.3).

Results of univariate analyses and the result of AICc model selection between RS and other parameters in the central, parafoveal, and extrafoveal areas are presented in Table 3. In the central area, no parameters were significantly related to RS using both perimetries.

In the parafoveal area, *VDs*, *VDd*, and *RV* were significantly correlated with *RS_W/W* and *RS_B/Y* (both $P<0.001$, linear mixed model). In the extrafoveal area, *VDs*, *VDd*, and *RV* were also correlated with *RS_W/W* and *RS_B/Y* (linear mixed model, $P=0.02$, $P=0.001$, and $P=0.02$ with W/W perimetry; $P=0.007$, $P<0.001$, and $P=0.01$ with B/Y perimetry, respectively). AICc model selection was conducted for *RS_W/W* and *RS_B/Y*. The optimal model for *RS_W/W* and *RS_B/Y* in the parafoveal area was as follows: $RS_W/W = 6.52 + 0.18 (\pm 0.03) \times VDd + 15.45 (\pm 4.63) \times RV$ (AICc = 539.9) and $RS_B/Y = -17.03 + 0.32 (\pm 0.05) \times VDd + 25.42 (\pm 7.12) \times RV$ (AICc = 635.4) (Table 3). Conversely, in the extrafoveal area, only *VDd* was included in the optimal models:

$$RS_W/W = 18.19 + 0.13(\pm 0.039) \times VDd(\text{AICc} = 602.3)$$

$$RS_B/Y = 1.94 + 0.26(\pm 0.054) \times VDd(\text{AICc} = 675.4)$$

	Univariate				Multivariate		
	Variables	Estimate	SE	P value	Estimate	SE	P value
Parafovea RS_W/W	Age	-0.068	0.036	0.067	N.S	N.S	N.S
	VDs	0.25	0.039	<0.001	N.S	N.S	N.S
	VDd	0.24	0.029	<0.001	0.19	0.032	<0.001
	RV	28.09	4.91	<0.001	14.18	4.86	0.004
Parafovea RS_B/Y	Age	-0.11	0.067	0.10	N.S	N.S	N.S
	VDs	0.38719	0.064	<0.001	N.S	N.S	N.S
	VDd	0.40	0.046	<0.001	0.33	0.05	<0.001
	RV	46.15	8.09	<0.001	23.6	7.71	0.002
Extrafovea RS_W/W	Age	-0.070	0.046	0.14	N.S	N.S	N.S
	VDs	0.11	0.047	0.022	N.S	N.S	N.S
	VDd	0.12	0.037	0.001	0.12	0.037	0.002
	RV	5.63	2.45	0.024	N.S	N.S	N.S
Extrafovea RS_B/Y	Age	-0.11	0.073	0.14	N.S	N.S	N.S
	VDs	0.18	0.066	0.007	N.S	N.S	N.S
	VDd	0.22	0.052	<0.001	0.22	0.052	<0.001
	RV	8.72	3.42	0.012	N.S	N.S	N.S
Center RS_W/W	Age	-0.026	0.058	0.66	N.S	N.S	N.S
	VDs	0.060	0.089	0.51	N.S	N.S	N.S
	VDd	0.084	0.075	0.27	N.S	N.S	N.S
	RV	-5.31	20.08	0.79	N.S	N.S	N.S
Center RS_B/Y	Age	-0.059	0.10	0.56	N.S	N.S	N.S
	VDs	0.16	0.15	0.30	N.S	N.S	N.S
	VDd	0.042	0.13	0.76	N.S	N.S	N.S
	RV	27.50	34.54	0.43	N.S	N.S	N.S

Table 3. Correlation between retinal sensitivity measured using both perimetries and other parameters. SE standard error, RS_W/W retinal sensitivity in white-on-white perimetry, RS_B/Y retinal sensitivity in blue-on-yellow perimetry, VDs vessel density in superficial capillary plexus, Dd vessel density in deep capillary plexus, RV retinal volume, N.S. not selected (linear mixed model, model selection using the second-order bias-corrected Akaike Information Criterion index).

The difference in RS between the BRVO-affected and unaffected areas using both perimetries is presented in Fig. 1. The difference in RS using B/Y perimetry was significantly larger than that using W/W perimetry in both the parafoveal and extrafoveal areas (paired *t*-test, $P < 0.001$ and $P = 0.008$, respectively). The result of AICc model selection for structural parameters is presented in Table 4. In both the parafovea and extrafovea, only RS_B/Y was included in the optimal model for VDd, with RS_W/W not being included (AICc = 758.1 and AICc = 798.9, respectively); inclusion of RS_W/W resulted in an increase in AICc values. In the parafovea as well, only RS_B/Y was included in the optimal model for RV (AICc = -384.9) and RS_W/W was not.

Discussion

In this study, RS was measured using the B/Y and W/W perimetries in eyes with resolved BRVO, along with measurements obtained using OCTA. Our results suggested that RS measured using B/Y perimetry had a tighter correlation with VDd and RV than RS measured using W/W perimetry. In addition, the results suggested that the difference in RS between the affected and unaffected areas in eyes with BRVO was larger with B/Y perimetry than with W/W perimetry. Taken together, our results suggest that retinal function in eyes with BRVO is better reflected with B/Y perimetry than with W/W perimetry.

This study showed that RV in the parafovea was the most important variable for BCVA, whereas VDd and VDs in the parafoveal area were not. Previous studies have found contradicting results on the association between BCVA and OCT parameters. A recent study has suggested that foveal avascular zone (FAZ) is correlated to VA in both eyes of patients with diabetic retinopathy and in eyes with BRVO¹⁴. In contrast, Kadomoto et al.¹⁵ have reported that FAZ is not correlated with VA, but parafoveal NPA in the DCP is strongly associated with VA and macular sensitivity. Wakabayashi et al.⁴ have reported that FAZ, microvascular abnormalities, and VD are related to visual function and that VD of DCP significantly correlates with BCVA measured using OCTA.

The reason behind this discrepancy is unknown, but it is attributable to the difference in data collection. Kadomoto et al. measured parafoveal NPA within 3×3 mm in each eye; Wakabayashi et al. measured retinal perfusion area within 3×3 mm, whereas we measured VD by dividing the parafoveal region into four parts.

However, when we calculated VD and RS within the total 3×3 -mm area, only RV was negatively correlated to the logarithm of the minimum angle resolution (logMAR) VA (linear regression, $P = 0.015$) and VDd was

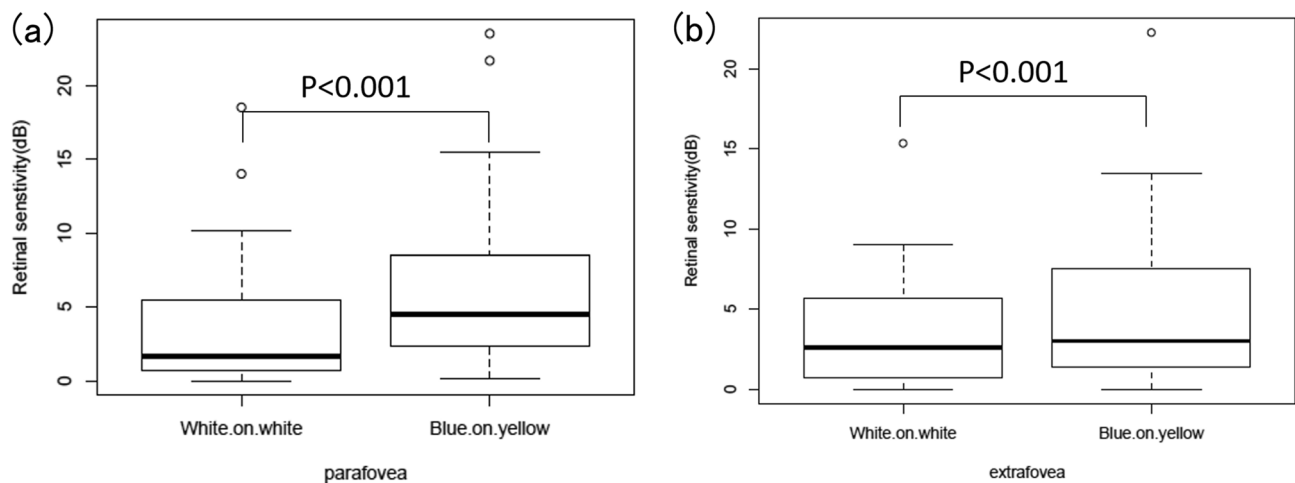


Figure 1. Comparison of the difference in RS between the BRVO-affected and unaffected areas using both perimetries. **(a)** Comparison in the parafovea, **(b)** comparison in the extrafovea. The difference with B/Y perimetry was significantly larger than that with W/W perimetry in both regions (the paired Student's *t* test). The images were generated using R software version 3.5.2, following the guideline (<https://cran.r-project.org/doc/FAQ/R-FAQ.html#Citing-R>). RS retinal sensitivity, BRVO branch retinal vein occlusion, B/Y blue on yellow, W/W white on white.

	Variables	Estimate	Standard error	P value
Parafovea VDd	RS_W/W	N.S	N.S	N.S
	RS_B/Y	0.99	0.11	< 0.001
Parafovea RV	RS_W/W	N.S	N.S	N.S
	RS_B/Y	0.0045	0.00084	< 0.001
Extrafovea VDd	RS_W/W	N.S	N.S	N.S
	RS_B/Y	0.58	0.15	< 0.001

Table 4. AICc model selection evaluating parameters that are important for VDd and RV. AICc second-order bias-corrected Akaike Information Criterion, RS_W/W retinal sensitivity in white-on-white perimetry, RS_B/Y retinal sensitivity in blue-on-yellow perimetry, VDd vessel density in deep capillary plexus, RV retinal volume (linear mixed model, model selection using AICc).

not. Conversely, among RV, VDd, and VDs, only VDd was selected as an explanatory variable of RS_W/W and RS_B/Y (linear regression, $P < 0.0001$, respectively).

The present study demonstrated that VDd is an explanatory variable of RS in both perimetries but VDs is not. Previous studies have reported that microvascular abnormalities, such as capillary telangiectasia, microaneurysm, collateral vessels, and FAZ enlargement, are more frequently observed in DCP than in SCP^{16–21}. Moreover, Birol et al. have reported that capillary deep layer provides 10–15% of oxygen supply to the photoreceptor cells²²; hence, ischemia in DCP may gradually influence photoreceptor integrity^{23,24}, which is significantly associated with visual outcomes of BRVO^{25,26}. Based on the results of this study and previous studies, it is suggested that the perfusion status of DCP compared with that of SCP is more important for RS.

In this study, RS measured with B/Y perimetry compared with that measured with W/W perimetry was more closely associated with VDd and RV. In addition, the difference in RS between the BRVO-affected and unaffected areas was significantly larger with B/Y perimetry than with W/W perimetry, which may be because compared with the long- and medium-wavelength-sensitive cones, the short-wavelength-sensitive cones and their neural connections are more vulnerable to damage caused by lack of oxygen^{27–29}. Indeed, previous clinical studies have reported that abnormality with B/Y perimetry occurs at the early stage of diabetic retinopathy than that with W/W perimetry, which is considered as subclinical retinal hypoxia secondary to hyperglycemia^{12,30–33}. Smith et al. also reported that experimental hypoxia preferentially led to blue–yellow abnormality in a psychophysiological test using the FM 100-hue test³⁴. Our result is attributable to the fact that the number of short-wavelength-sensitive cones is much smaller than that of long- and medium-wavelength-sensitive cones in the macular region.

In the real-world setting, functional assessment of BRVO is usually performed on the basis of BCVA, with perimetric examinations being only rarely conducted. In contrast, several previous studies have suggested the usefulness of measuring RS using W/W perimetry in eyes with BRVO. For instance, some studies have suggested the usefulness of this approach in detecting early and subtle functional damage in eyes with BRVO^{5,35–37}. In addition, clinically, it is often observed that patients with resolved BRVO describe visual symptoms such as decreased RS, metamorphopsia, and central scotoma that cannot be fully explained solely on the basis of BCVA.

The present study suggests a further greater merit on the use of B/Y perimetry in measuring such pathologies in eyes with BRVO.

This study has several limitations. First, the study has a retrospective nature, and the number of examined eyes was relatively small. Second, to compare 6-mm ETDRS grid, we measured VF only within 10°, and VF did not cover the whole BRVO-affected area. Evaluation of RS in a wider area may be further advantageous to assess the structure–function relationships in BRVO.

In conclusion, we found that VDD and RV are more strongly correlated to RS_{B/Y} than to RS_{W/W}. Moreover, the difference in RS between BRVO-affected and unaffected areas was significantly larger with B/Y perimetry than with W/W perimetry. These findings indicate that it is useful to assess RS using B/Y perimetry in eyes with BRVO.

Methods

This study was approved by the Research Ethics Committee of the Graduate School of Medicine and Faculty of Medicine at The University of Tokyo. Written informed consent was obtained from the patients for their information to be stored in the hospital database and used for research. The study protocol was in accordance with the Declaration of Helsinki.

Subjects. The study included 29 eyes (15 right and 14 left eyes) of 29 patients with resolved BRVO, who were examined at the Department of Ophthalmology of the University of Tokyo Hospital. All eyes had received antivascular endothelial growth factor therapies. Macular edema and serous retinal detachment were completely resolved as shown by careful examination using OCT macular scans. Eyes with other ophthalmic diseases, such as epiretinal membrane, glaucoma, and diabetic retinopathy, and eyes that had undergone photocoagulation therapy were excluded. Eyes with cataract, which could hinder VF measurement, were excluded.

All patients had undergone comprehensive ophthalmologic examinations such as BCVA, slit-lamp biomicroscopy, intraocular pressure, and indirect fundus ophthalmoscopy. In addition, measurements using W/W perimetry, B/Y perimetry, OCT, and OCTA were performed the same day, as detailed below.

Visual field test. Each patient underwent W/W and B/Y VF testing using AP-7000 (Kowa, Tokyo, Japan). Both VF test measurements were performed applying the 10-2 test grid using the Goldmann size III target. W/W and B/Y perimetry measurements were performed in a random order. Both VF tests were performed using the Quick 1 algorithm, which reportedly has outcomes similar to those obtained using the Swedish interactive threshold algorithm standard test³⁸. B/Y perimetry was performed under a 450-nm narrow band target on a bright broad band 100 cd/m² against a yellow background (600 nm). We confirmed that all of the VF measurements satisfied the reliability criteria, defined as a fixation loss rate of <20%, false-positive rate of <15%, and false-negative rate of <33%.

OCT measurement. All the patients underwent macular topographic mapping under raster scan protocol using Spectral Domain OCT (SPECTRALIS OCT, Heidelberg Engineering, Heidelberg, Germany). The raster scan was performed using 25 B-scans (768 A-scans per B-scan) of a 30° × 20° area. Analysis of RV with a 6-mm ETDRS grid was automatically performed using SPECTRALIS OCT built-in software.

OCTA measurement and vessel density. OCTA was performed using Avanti RTVue XR (Optovue, Fremont, CA). The scanning area was captured in 6 × 6-mm sections centered on the fovea. To obtain images of SCP, the SCP slab was taken from the internal limiting membrane (offset, 3 μm) to the inner plexiform layer (offset, 15 μm). To obtain images of DCP, the DCP slab was taken from the inner plexiform layer (offset, 15 μm) to the outer plexiform layer (offset, 70 μm). To evaluate the capillary perfusion status of SCP and DCP, binarized *en face* images were prepared using ImageJ software (ImageJ, V.2.0.0-rc-69/1.52i, NIH, Bethesda, Maryland, USA). A modified Niblack's method was used to perform binarization of each *en face* image, similar to our previous study³⁹. Briefly, the image was converted to 8 bits and adjusted using the Niblack auto local threshold. Then, we set the regions of interest that were each of the nine macular regions in a 6-mm-diameter circle that was centered on the fovea, as defined in ETDRS (Fig. 2). We defined the center circle of 1-mm diameter on the fovea as the center, a 3-mm-diameter concentric circle as the parafovea, and a 6-mm-diameter concentric circle as the extrafovea. The mean gray value was calculated for each of the nine macular regions and was defined as VD.

Mapping VF to OCT/OCTA images. To analyze each section of the ETDRS grid, we assigned the measurement thresholds for all 68 points to the nine regions of the ETDRS grid and calculated the mean values of points that were assigned to each of the nine regions as a guide (Fig. 3). The OCT analysis region (6 mm) and the 10-2 measurement region were considered to be equivalent; analysis was performed in the range corresponding to each of the nine regions of the ETDRS grid.

Comparison of RS between BRVO-affected and unaffected areas. In this study, all the patients had been carefully examined by ophthalmologists and confirmed to have BRVO in only one eye. Difference in RS between the defective and nondefective parts was compared using both perimetries. In the parafovea, the difference in RS between the inner–superior and inner–inferior areas was calculated using both W/W and B/Y perimetries. In the extrafovea, the difference between the outer–superior and outer–inferior areas was calculated (Fig. 4). Other areas were excluded in this analysis because BRVO-affected and unaffected areas were mixed.

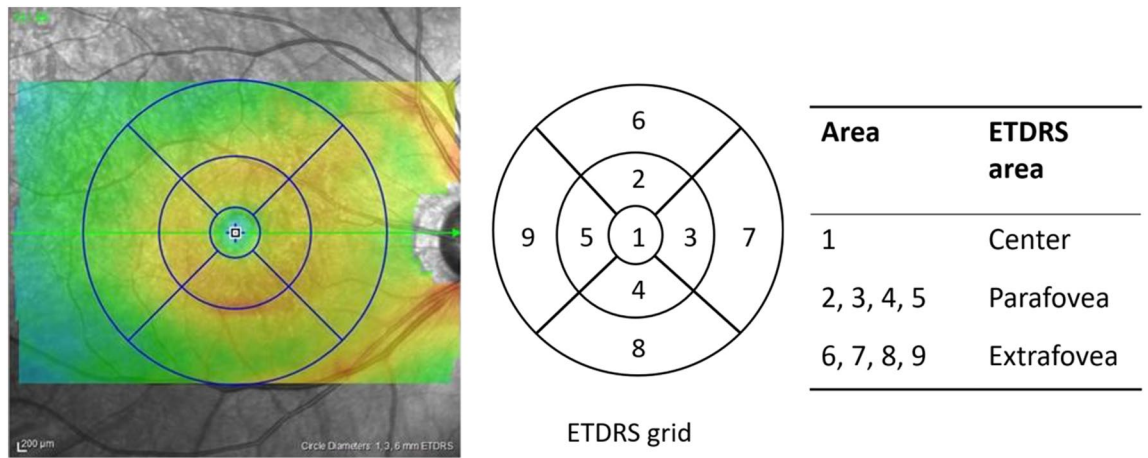


Figure 2. Sectorization of the macula. The built-in OCT software automatically analyzed the mean retinal thickness and volume in each of the nine macular regions in a 6-mm-diameter circle that was centered on the fovea, as defined in ETDRS. The diameter of the central circle was 1 mm, that of the inner ring was 3 mm, and that of the outer ring was 6 mm. The center circle was defined as the center, the inner ring as the parafovea, and the outer ring as the extrafovea. *VF* visual field, *ETDRS* Early Treatment of Diabetic Retinopathy Study.

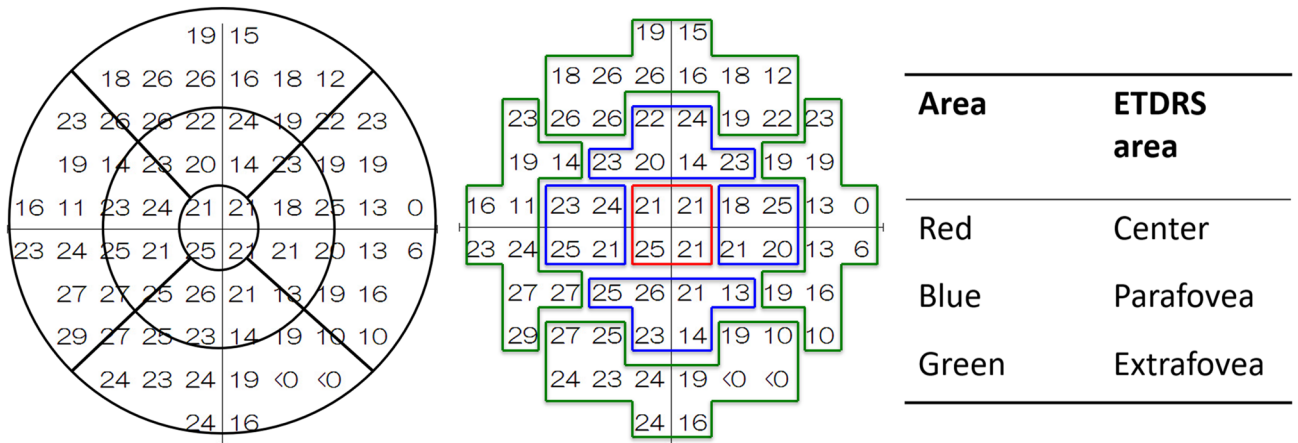


Figure 3. Mapping of VF. All 68 points were assigned to each of the nine regions after ETDRS⁴⁰. The mean retinal sensitivity was calculated in each sector. *OCT* optical coherence tomography.

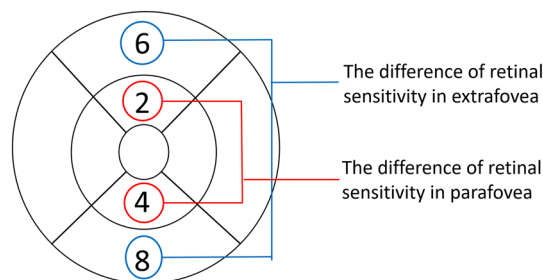


Figure 4. Comparison of the RS between BRVO-affected and unaffected areas. In the parafovea, the difference between areas 2 and 4 was calculated using both B/Y and W/W perimetries. In the extrafovea, the difference between areas 6 and 8 was calculated. *RS* retinal sensitivity, *B/Y* blue on yellow, *W/W* white on white, *BRVO* branch retinal vein occlusion.

Statistical analysis. BCVA was measured in decimal units and converted to logMAR units for statistical analyses. Univariate and multivariate analyses were performed to investigate the correlation between OCT parameters and BCVA, RS_W/W, and RS_B/Y. This analysis was followed by model selection using the AICc index. In a multivariate regression model, degrees of freedom decrease with an increase in the number of variables; hence, the use of model selection methods is recommended to improve the model fit by removing redundant variables, particularly when the number of explanatory variables is large, rather than performing simple multivariate regression analysis^{41,42}. Using model selection with AICc, the model with the smallest AICc value was selected as the optimal model. AIC is an established statistical measure used to evaluate the relationship between variables, and AICc is a corrected form of AIC, providing accurate estimation even when the sample size is small⁴³. The difference in RS between the BRVO-affected and unaffected areas was compared between W/W and B/Y perimetries using paired Student's *t* test.

R statistical software version 3.5.2 (The R Foundation for Statistical Computing, Vienna, Austria) was used for all analyses.

Received: 16 June 2020; Accepted: 4 November 2020

Published online: 17 November 2020

References

1. Group, B. Argon laser scatter photocoagulation for prevention of neovascularization and vitreous hemorrhage in branch vein occlusion. A randomized clinical trial. *Arch Ophthalmol.* **104**, 34–41 (1986).
2. Tsai, G., Banaee, T., Conti, F. F. & Singh, R. P. Optical coherence tomography angiography in eyes with retinal vein occlusion. *J. Ophthalmic. Vis. Res.* **13**, 315–332 (2018).
3. Kuehlewein, L., An, L., Durbin, M. K. & Sadda, S. R. Imaging areas of retinal nonperfusion in ischemic branch retinal vein occlusion with swept-source OCT microangiography. *Ophthalmic. Surg. Lasers Imaging Retina* **46**, 249–252 (2015).
4. Wakabayashi, T. *et al.* Retinal microvasculature and visual acuity in eyes with branch retinal vein occlusion: Imaging analysis by optical coherence tomography angiography. *Invest. Ophthalmol. Vis. Sci.* **58**, 2087 (2017).
5. Manabe, S. *et al.* Association between parafoveal capillary nonperfusion and macular function in eyes with branch retinal vein occlusion. *Retina* **37**, 1731–1737 (2017).
6. De Jong, L. A., Snepvangers, C. E., van den Berg, T. J. & Langerhorst, C. T. Blue-yellow perimetry in the detection of early glaucomatous damage. *Doc. Ophthalmol.* **75**, 303–314 (1990).
7. Sample, P. A., Taylor, J. D., Martinez, G. A., Lusky, M. & Weinreb, R. N. Short-wavelength color visual fields in glaucoma suspects at risk. *Am. J. Ophthalmol.* **115**, 225–233 (1993).
8. Johnson, C. A., Adams, A. J., Casson, E. J. & Brandt, J. D. Blue-on-yellow perimetry can predict the development of glaucomatous visual field loss. *Arch. Ophthalmol.* **111**, 645–650 (1993).
9. Hudson, C. *et al.* Short-wavelength sensitive visual field loss in patients with clinically significant diabetic macular oedema. *Diabetologia* **41**, 918–928 (1998).
10. Lobefalo, L. *et al.* Blue-on-yellow and achromatic perimetry in diabetic children without retinopathy. *Diabetes Care* **21**, 2003–2006 (1998).
11. Keltner, J. L. & Johnson, C. A. Short-wavelength automated perimetry in neuro-ophthalmologic disorders. *Arch. Ophthalmol.* **113**, 475–481 (1995).
12. Afrashi, F., Erakgün, T., Köse, S., Ardic, K. & Menteş, J. Blue-on-yellow perimetry versus achromatic perimetry in type 1 diabetes patients without retinopathy. *Diabetes Res. Clin. Pract.* **61**, 7–11 (2003).
13. Afrashi, F. *et al.* Comparison of achromatic and blue-on-yellow perimetry in patients with resolved central serous chorioretinopathy. *Ophthalmologica* **219**, 202–205 (2005).
14. Balaratnasingam, C. *et al.* Visual acuity is correlated with the area of the foveal avascular zone in diabetic retinopathy and retinal vein occlusion. *Ophthalmology* **123**, 2352–2367 (2016).
15. Kadomoto, S. *et al.* Evaluation of macular ischemia in eyes with branch retinal vein occlusion: an optical coherence tomography angiography study. *Retina* **38**, 272–282 (2018).
16. Suzuki, N. *et al.* Microvascular abnormalities on optical coherence tomography angiography in macular edema associated with branch retinal vein occlusion. *Am. J. Ophthalmol.* **161**, 126–132.e1 (2016).
17. Coscas, F. *et al.* Optical coherence tomography angiography in retinal vein occlusion: Evaluation of superficial and deep capillary plexa. *Am. J. Ophthalmol.* **161**, 160–171.e2 (2016).
18. Rispoli, M., Savastano, M. C. & Lumbroso, B. Capillary network anomalies in branch retinal vein occlusion on optical coherence tomography angiography. *Retina (Philadelphia Pa.)* **35**, 2332–2338 (2015).
19. Adhi, M. *et al.* Retinal capillary network and foveal avascular zone in eyes with vein occlusion and fellow eyes analyzed with optical coherence tomography angiography. *Invest. Ophthalmol. Vis. Sci.* **57**, OCT486–494 (2016).
20. Kang, J.-W., Yoo, R., Jo, Y. H. & Kim, H. C. Correlation of microvascular structures on optical coherence tomography angiography with visual acuity in retinal vein occlusion. *Retina* **37**, 1700–1709 (2017).
21. Freund, K. B. *et al.* Association of optical coherence tomography angiography of collaterals in retinal vein occlusion with major venous outflow through the deep vascular complex. *JAMA Ophthalmol.* **136**, 1262 (2018).
22. Birol, G., Wang, S., Budzynski, E., Wangsa-Wirawan, N. D. & Linsenmeier, R. A. Oxygen distribution and consumption in the macaque retina. *Am. J. Physiol. Heart. Circ. Physiol.* **293**, H1696–1704 (2007).
23. Scarinci, F., Jampol, L. M., Linsenmeier, R. A. & Fawzi, A. A. Association of diabetic macular nonperfusion with outer retinal disruption on optical coherence tomography. *JAMA Ophthalmol.* **133**, 1036–1044 (2015).
24. Scarinci, F., Nesper, P. L. & Fawzi, A. A. Deep retinal capillary nonperfusion is associated with photoreceptor disruption in diabetic macular ischemia. *Am. J. Ophthalmol.* **168**, 129–138 (2016).
25. Domalpally, A. *et al.* Association of outer retinal layer morphology with visual acuity in patients with retinal vein occlusion: SCORE Study Report 13. *Eye (Lond)* **26**, 919–924 (2012).
26. Ota, M. *et al.* Association between integrity of foveal photoreceptor layer and visual acuity in branch retinal vein occlusion. *Br. J. Ophthalmol.* **91**, 1644–1649 (2007).
27. Sample, P. A. & Weinreb, R. N. Color perimetry for assessment of primary open-angle glaucoma. *Invest. Ophthalmol. Vis. Sci.* **31**, 1869–1875 (1990).
28. Ham, W. T., Mueller, H. A., Ruffolo, J. J., Guerry, D. & Guerry, R. K. Action spectrum for retinal injury from near-ultraviolet radiation in the aphakic monkey. *Am. J. Ophthalmol.* **93**, 299–306 (1982).
29. Johnson, C. A., Adams, A. J., Twelker, J. D. & Quigg, J. M. Age-related changes in the central visual field for short-wavelength-sensitive pathways. *J. Opt. Soc. Am. A* **5**, 2131–2139 (1988).

30. Nitta, K., Saito, Y., Kobayashi, A. & Sugiyama, K. Influence of clinical factors on blue-on-yellow perimetry for diabetic patients without retinopathy: Comparison with white-on-white perimetry. *Retina* **26**, 797–802 (2006).
31. Daley, M. L., Watzke, R. C. & Riddle, M. C. Early loss of blue-sensitive color vision in patients with type I diabetes. *Diabetes Care* **10**, 777–781 (1987).
32. Greenstein, V., Sarter, B., Hood, D., Noble, K. & Carr, R. Hue discrimination and S cone pathway sensitivity in early diabetic retinopathy. *Invest. Ophthalmol. Vis. Sci.* **31**, 1008–1014 (1990).
33. Yamamoto, S., Kamiyama, M., Nitta, K., Yamada, T. & Hayasaka, S. Selective reduction of the S cone electroretinogram in diabetes. *Br. J. Ophthalmol.* **80**, 973–975 (1996).
34. Smith, V. C., Ernest, J. T. & Pokorny, J. Effect of hypoxia on FM 100-Hue test performance. *Mod. Probl. Ophthalmol.* **17**, 248–256 (1976).
35. Imasawa, M., Iijima, H. & Morimoto, T. Perimetric sensitivity and retinal thickness in eyes with macular edema resulting from branch retinal vein occlusion. *Am. J. Ophthalmol.* **131**, 6 (2001).
36. Kriechbaum, K. *et al.* Association of retinal sensitivity and morphology during antiangiogenic treatment of retinal vein occlusion over one year. *Ophthalmology* **116**, 2415–2421 (2009).
37. Fujino, R. *et al.* The usefulness of the retinal sensitivity measurement with a microperimetry for predicting the visual prognosis of branch retinal vein occlusion with macular edema. *Graefes Arch. Clin. Exp. Ophthalmol.* <https://doi.org/10.1007/s00417-020-04759-9> (2020).
38. Udagawa, S. *et al.* Comparison of the glaucoma diagnostic capability and other parameters of KOWA AP-7000TM and Humphrey field analyzer. *Nippon Ganka Gakkai Zasshi* **121**, 915–922 (2017).
39. Hashimoto, Y. *et al.* A novel method for the objective identification of hyperautofluorescent ring in retinitis pigmentosa using binarization processing. *Trans. Vis. Sci. Tech.* **8**, 20 (2019).
40. Early treatment diabetic retinopathy study design and baseline patient characteristics. ETDRS report number 7. *Ophthalmology* **98**, 741–756 (1991).
41. Tibshirani, R. J. & Taylor, J. Degrees of freedom in lasso problems. *Ann. Statist.* **40**, 1198–1232 (2012).
42. Mallows, C. L. Some comments on C p. *Technometrics* **15**, 661–675 (1973).
43. Burnham, K. P. & Anderson, D. R. Multimodel inference: Understanding AIC and BIC in model selection. *Sociol. Methods Res.* **33**, 261–304 (2004).

Author contributions

K.A., T.I. and R.A. wrote the main manuscript. K.A. prepared figures and tables. Y.H. advised the statistical analysis. All authors contributed to the manuscript.

Competing interests

The authors declare no competing interests.

Additional information

Supplementary information is available for this paper at <https://doi.org/10.1038/s41598-020-77025-x>.

Correspondence and requests for materials should be addressed to T.I.

Reprints and permissions information is available at www.nature.com/reprints.

Publisher's note Springer Nature remains neutral with regard to jurisdictional claims in published maps and institutional affiliations.



Open Access This article is licensed under a Creative Commons Attribution 4.0 International License, which permits use, sharing, adaptation, distribution and reproduction in any medium or format, as long as you give appropriate credit to the original author(s) and the source, provide a link to the Creative Commons licence, and indicate if changes were made. The images or other third party material in this article are included in the article's Creative Commons licence, unless indicated otherwise in a credit line to the material. If material is not included in the article's Creative Commons licence and your intended use is not permitted by statutory regulation or exceeds the permitted use, you will need to obtain permission directly from the copyright holder. To view a copy of this licence, visit <http://creativecommons.org/licenses/by/4.0/>.

© The Author(s) 2020